Precise, Energy-Efficient Data Acquisition Architecture for Monitoring Radioactivity using Self-Sustainable Wireless Sensor Nodes

Andres Gomez, Michele Magno, Marie Francine Lagadec, Luca Benini
Integrated Systems Laboratory, ETH Zurich, Switzerland
Email: {firstname.lastname}@iis.ee.ethz.ch

***Abstract*—Measuring radiation dosage rates is becoming more and more important in many applications scenarios. Continuously monitoring radiation in contaminated and poorly accessible areas is challenging due to the frequent data collection/transmission combined with long life requirements. We present a self-sustainable wireless sensor node for low power, high precision radiation dosage rate monitoring. We propose an energy-efficient data acquisition algorithm that can reduce the energy per measurement, while guaranteeing minimal loss of precision. The proposed node is designed to work in collaboration with an unmanned aerial vehicle used for two essential mission steps: air-deployment of the wireless sensor nodes at suitable locations, and acquiring data logs via low-power, short-range radio communication in fly-by mode after a wake-up command. The system uses off-the-shelf components for defining the mission, drop-zone and trajectory, for compressing data and managing communication. The node is equipped with a novel low-power nuclear radiation sensor, and has been designed and implemented with self-sustainability in mind as it will be deployed in hazardous, inaccessible areas. To this end, the proposed node uses a combination of complementary techniques: a low-power microcontroller with non-volatile memory, energy harvesting, adaptive power management and a nano-watt wake-up radio. Experimental results demonstrate the precision and the low energy consumption of the radiation sensor, the energy efficiency of the whole solution and the acquisition algorithms. The node consumes only 31 μW in sleep mode and 1.7 mW in active mode, and has the capability to achieve perpetual monitoring once deployed.**

I. Introduction

The continuous monitoring of ambient radioactivity over widely contaminated areas has become a hot topic, as dramatically illustrated in the aftermath of the Fukushima Daiichi nuclear power plant incident in March 2011 [1]. However, conventional radioactivity monitoring systems face severe drawbacks when having to continuously monitor an extensive, inaccessible, and hazardous area. In fact, they generally cannot be deployed safely, quickly and effectively in potentially contaminated areas, as there may be physical obstacles, a lack of communication infrastructure, and an unknown level of exposure. Their deployment is not automated, further increasing potential human exposure, or is restricted to ground robots with limitations in terms of speed and coverage area. As a result, most systems are generally not economically viable in terms of installation, operation, maintenance and mission fulfillment

Wireless sensor networks (WSNs) have become a mature technology for a wide range of applications, among them environmental monitoring, health care, security, and industrial surveillance, mainly thanks to the flexible distribution of WSN nodes [2]–[4]. WSNs offer a new approach to the challenge of ambient radioactivity monitoring, as they eliminate the dependence on in-place communication and on-site manpower [5]. On the other hand, the operational lifetime of the WSNs individual sensor nodes is limited by energy constraints, as wireless sensor nodes are commonly powered by batteries. Power consumption for long term monitoring is an even more critical constraint when applications require long-range communication technologies (e.g., GSM, WLAN) and/or power-hungry devices such as Geiger-Müller counters, traditionally used as radioactivity sensors [6].

To overcome the obstacle of power consumption in long-range communication, novel approaches which combine WSN with Unmanned Aerial Vehicles (UAV) or Micro Aerial Vehicles (MAV) are gaining increased attention, due to their potential for reducing the power consumption of long-range communication and for accessing hazardous areas. In these new systems, there is a clear separation between the short-distance communication of the WSN and the long-range communication performed by the UAV vehicles, once they have collected data from the WSN [7]–[10]. New technologies can further reduce power consumption by limiting the radio activities to their strict minimum, as is the case with a wake-up radio (WUR) [11], or dynamically reducing the sensor's sample rate when the battery level becomes critically low to guarantee the self-sustainability of the nodes in applications where their inaccessibility prohibits a change of batteries. Finally, energy harvesting (EH) is becoming an established method for enabling long term monitoring by WSN and has been employed in several applications involving self-powered systems [12]–[15]. As is always the case with EH, it is important that energy availability be tied to the application scenario [16], [17]. The choice of a solar panel presumes the availability of sunlight, which can be guaranteed by a careful planning of the UAV's sensor deployment.

New criteria are needed in the hardware and software design of both the nodes and their communication. Combining low-power design, power management techniques and EH increases network lifetime by several orders of magnitude compared with conventional WSN, due to increased energy availability and reduced power consumption [18]–[20]. Node networks

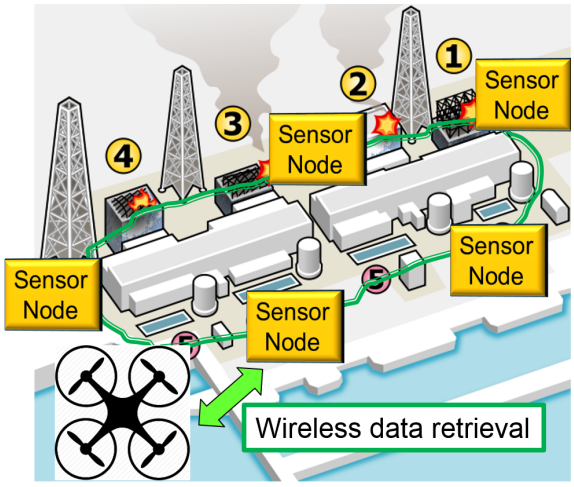

Figure 1: Proposed UAV and Sensor Node WSN for Radiation Monitoring.

with a very long or even unlimited operating life become feasible. There is, of course, a trade-off between effective energy management and monitoring quality [21].

In this paper, a novel ultra-low power, off-the-shelf radiation sensor is presented and tested with different radiation dosage rates in order to optimize the acquisition algorithm in terms of energy efficiency. We describe the design, the implementation and testing of a small form factor self-powered wireless sensor node suitable for deployment by UAV for dosage rate monitoring in contaminated areas. An overview of the UAV/sensor node network can be seen in Figure 1. The node, using a +3dBi antenna, can store dosage rate readings until the UAV is within a 50m radius. At this point, the node can detect a wake-up signal, turn on power-hungry data radio and transmit the stored data to the UAV.

- The design and implementation of a self-sustainable wireless sensor node for monitoring radioactivity.
- Experimental characterization of a novel solid-state radiation sensor and data acquisition algorithm under controlled dosage rates.
- We demonstrate the node's self-sustainability by simulation, after measuring the energy intake of a solar panel in an outdoor environment and the power consumption of our proposed energy efficient data acquisition algorithm.

The remainder of the paper is organized as follows. Related work is presented in Sec. 2. The proposed sensor node's architecture is discussed in detail in Sec. 3. The radiation sensor's characterization and our proposed energy optimized data acquisition are presented in Sec. 4 and 5, respectively. Sec. 6 presents the experimental results for the combined system and simulation for evaluating the self-sustainability and energy efficiency of the proposed solution. Finally, we conclude our work in Sec. 7.

[0]Image adapted from: http://bit.ly/2rxX1VI

II. Related Works

Research on WSNs has been very prolific in recent years with a variety of solutions in a wide range of application scenarios. There are many examples of implemented and deployed WSNs that exploit intelligent sensing, wireless communication and computing abilities to monitor environmental phenomena [1]. In this area, WSNs have recently been regarded as a promising candidate to monitor nuclear radiation in contaminated or dangerous areas, especially for nuclear power plants [5]–[7]. Nuclear radiation has typically been detected via hand-held Geiger-Müller counters, which are particularly suited for detecting radioactivity via the strongly ionizing effect of alpha particles [6]. Geiger-Müller Counters (GMC) can also be used for radioactivity detection in autonomous WSN sensor nodes [22]. Zigbee networks with GMC's have been used to monitor radiation levels in nuclear facilities [23]. However, the limitations of using GMCs in terms of size (mainly dictated by the tube length), weight, cost and power consumption make them a poor choice for miniaturized, low-energy, low-cost sensor nodes. In our design, a novel nuclear radiation sensor [24] based on an array of customized PIN diodes is used. The sensor is capable of detecting beta radiation, gamma radiation and X-rays with very low power requirements.

Another major challenge in WSNs is the limited energy storage capacity in the node, usually in the form of batteries or supercapacitors. The use of energy harvesters in combination with energy storage elements attempts to overcome this issue, and in some applications even achieves self-sustainability [21]. To achieve this, sensor nodes need to limit their consumption to the average, long-term, harvested energy. Since the amount of harvested energy cannot be controlled, designers are limited to choosing packet acquisition and transmission schedules. To do this optimally, offline solutions assume the nodes have full knowledge of the harvesting and information generation processes, while online approaches can only rely on some prior statistical knowledge [25]. Researchers have been very active in this field, and many promising approaches are presented in literature [12], [13], [26]. In applications where wireless sensor nodes monitoring contaminated areas are expected to operate long-term without human maintenance, Energy Harvesting (EH) is essential. As they usually imply an outdoor setting, the most commonly available ambient energy sources are photovoltaic, wind turbine or mechanical energy (harvesting from vibrations or strain) [14]. Photovoltaic energy harvesters are the most mature technology to achieve self-sustainability in outdoor scenarios when the system is well designed and dimensioned. In this paper, we target self-sustainability using a photovoltaic cell and a commercial integrated circuit for power management with a small form factor, which guarantee state-of-the-art performance in terms of efficiency and adaptive power management.

Another important issue for WSN in wide and poorly accessible areas is the node's deployment and the collection of data from the base station [27]. Some approaches use GSM band [1], but these approaches are expensive in terms of

cost and power, and it is not always possible to guarantee network coverage. Due to their flexibility and cost-reduction potential, the use of UAVs for sensor network deployment has been studied for many years [26]. In [7], the authors developed a system for the cooperation of UAV, static nodes, and mobile nodes, where GPS was used for position estimation. The authors described communication issues between nodes after deployment due to their positioning. Another approach is to use the UAVs not for sensor deployment, but for actually monitoring the area itself [28]. This approach can be challenging since the relatively short lifetimes of UAV's prevent them from continuously monitoring an area though EH alone. Besides the use of UAVs, sensor network deployment using unmanned ground vehicles has also received considerable attention from the research community. Data collection from unmanned explorations or monitoring have also been proposed [29]. The approach presented in [8] is similar to the one proposed in this paper, however, the authors do not use any power management and EH, and the ground network does not achieve self-sustainability. Moreover, the radio activities are very expensive in terms of power (using Bluetooth or similar power hungry communication) and no low-power mechanisms are used, rendering it unsuitable for long-term self-sustainable monitoring. In this paper, we present a self-sustainable sensor node that can work in combination with UAV and is able to monitor radiation levels. To the best of our knowledge, there are no research-oriented or market products that offer similar functionalities to the ones proposed by our system.

III. System Design

The proposed system can be conceptually divided in two parts. The first part is the hardware architecture of the node, comprising a microcontroller, a radio chip and a Wake-Up Radio (WUR), harvester circuits and a radiation sensor. The second part is the software side, where we propose an energy-efficient, dynamic data acquisition algorithm to calculate the radiation dosage rates from the sensor output. Moreover, the power management techniques to reduce the total energy consumption and extend the node's lifetime are performed by software exploiting the hardware capabilities of the node (WUR and low power modes).

Figure 2 shows the block diagram of the developed wireless sensor node with its four main units: the sensor subsystem with the Teviso RD3024 sensor, the power management unit, in charge of harvesting energy, recharging the supercapacitor and powering the node, the ultra-low power microcontroller unit with non-volatile memory, and finally the communication unit which uses an ultra-low power WUR [30], [31] in sleep mode to detect the UAV's presence and the CC1100L as the main transceiver.

1) Energy Harvesting: To achieve self-sustainability, a system needs to have energy harvesting (EH) capabilities. For our application scenario, Sanyo's AM-1417 solar panel is able to provide enough energy for continued operation despite its small form factor (11.7mm x 35.0mm). The P-V characterization of the selected solar panel can be seen in Figure 3. It can

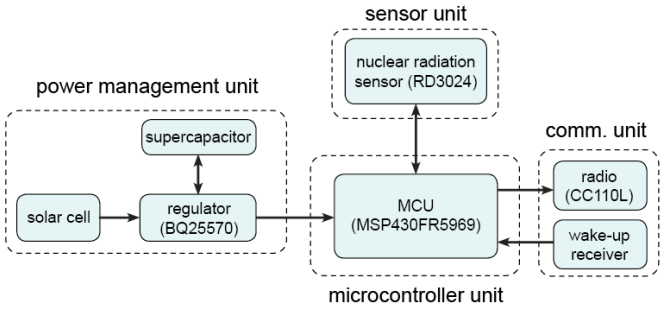

Figure 2: Sensor Node Architecture

be seen that under good lighting conditions, i.e., a luminosity of 10,000 lux, the panel can generate a maximum power of 0.85 mW. To have the maximum power transfer at different operating conditions and load impedances, the BQ25570 energy harvester circuit was used. A 1 F supercapacitor has been used for storage, which will be charged to a maximum of 5.25 V. Due to the BQ's buck converter regulating the load's voltage (V_{load}=3.3 V), only 8 J of usable energy are stored between the maximum and operating voltages.

2) Microcontroller unit: The MSP430FR5969 from Texas Instruments was selected as the main core due to its ultra-low power consumption and 64KB FRAM, a novel fast on-chip non-volatile memory. The microcontroller acquires, processes, stores and sends the data via the radio when the UAV is ready to collect them.

3) Communication unit: The radio typically consumes a large amount of the total energy in a wireless sensor node. Consequently, any optimization that can be made in the communication system has a big impact on the node's self-sustainability requirements. In the proposed application, enabling asynchronous communication protocols significantly increases the energy efficiency of the communication, since the node can keep the radio in sleep to save power and turn it on it only when the UAV is near by. A broad variety of solutions for asynchronous low power receivers have been proposed addressing the main trade-off between power, range, and addressing capabilities [32]. One possibility is on-demand network flooding [33], where devices can send multi-hop

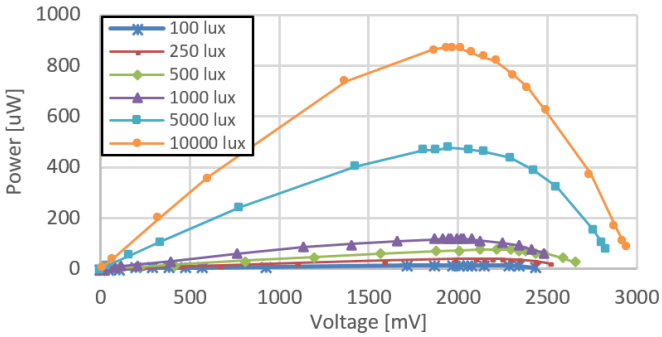

Figure 3: Solar Panel Characterization.

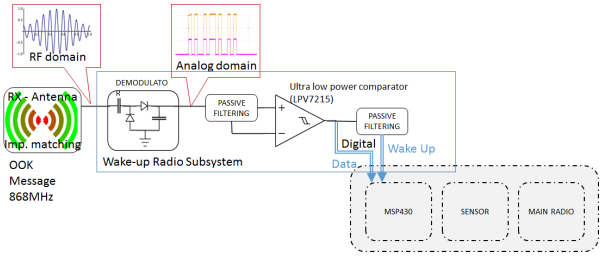

Figure 4: Nano-watt wake-up receiver architecture.

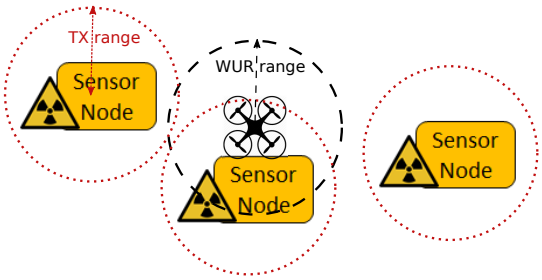

Figure 5: Network architecture comprised by several, non-overlapping sensor nodes. The range of the WUR is assumed to the be same as the TX radio.

messages with end-to-end latencies of tens of milliseconds. In this work we use single-hop communication, leveraging the CC110L for data transmission with an ultra-low power Wake-Up Radio (WUR). Figure 4 shows the architecture of the WUR, from [34].

The implemented receiver's power consumption was measured to be around 1 μW at 2V, with a sensitivity of -55 dBm [30]. Moreover, in-field experimental results demonstrate a range of 30 meters with a 3 dBi omnidirectional antenna.

4) Energy Efficient Communication Protocol: Figure 5 presents the architecture of the communication where the UAV can fly in a wide range field and the sensor node with the radiation sensors are deployed in the field. While the sensor node is in charge of collecting radiation data, the UAV collects the data from all the deployed sensors. In our scenario, we assume the nodes are deployed in the field in such a way that there is no overlap of the communication range (see Figure 5) so our application scenario does not require any addressing capabilities. Consequently, the node will spend most of its time in sleep mode, waking up only when the UAV is near by to collect data.

1) A timer expiration, to perform periodic sensing of the radiation sensor
2) The reception of the wake-up signal sent by the UAV and detected by the WUR

The first event, called data acquisition, will be explained in detail in Section 5. The second event, occurs when the UAV sends a signal to download the data logs from the sensor node. This wake-up signal is sent at 1 Kbps, since it's the data rate the WUR has been optimized for. If the UAV receives an acknowledgment (ACK) from a sensor node in its vicinity, it then reconfigures the data rate to 100Kbps to speed up the data transfer.

5) Radiation Sensor: Measuring levels of radioactivity typically requires the use of an accurate Geiger counter. However, these devices operate at a high voltage range (400-2,000V) [35] and require a Geiger-Müller tube containing an inert gas at low pressure. The Teviso RD3024 [24] solid state nuclear radiation sensor, used in our design, is based on customized PIN diodes which generate temperature compensated TTL pulses. It was chosen because of its low power consumption of only 400 μA at 3 V, small size and weight. It should be noted that, while the number of pulses per unit of time (given in counts per minute, or CPM) depends on the radiation level, the width of these pulses is variable. The width depends on how much of a ray's energy is absorbed by the diode's electron-hole pair. Figure 6 shows the sensor's response in terms of pulses per minute, on a logarithmic scale, with respect to the measured radiation dosage rate. In normal ambient conditions, radiation dosage rates are in the order of magnitude of 50-100 nSv/h. During radioactive emergencies, such as the Fukushima Daiichi nuclear power plant incident, the rates reached 2 mSv/h [1].

In order to measure the radiation dosage rate, the number of pulses generated by the sensor and the time taken to reach a statistically significant number of pulses need to be measured. According to the manufacturer, 1k samples are enough to have a statistically significant measurement. With these two values, the node is able to calculate the equivalent counts per minute, which can then be converted into a dosage rate in [mSv/h] units by multiplying the sensor's sensitivity. The dosage rate can be calculated either continuously, with a moving average, or it can be duty-cycled.

For a low-power, self-sustainable application, continuous sensing is too expensive, so one must periodically activate the sensor to make a measurement in a limited amount of time. However, if a stable measurement requires 1k samples, the settling time will vary greatly within the sensor's measurement range. When exposed to high dosage rates, much less time will be needed for the measurement to settle. These values and

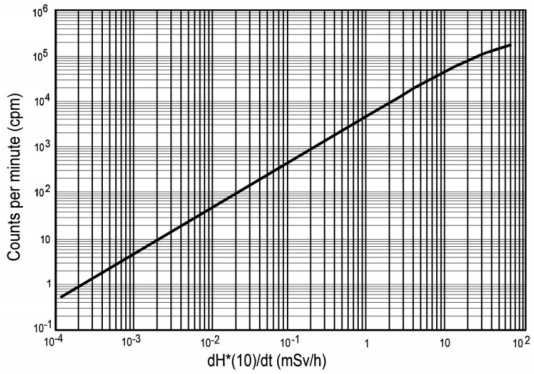

Figure 6: Sensor response as a function of the radiation dosage rate [24].

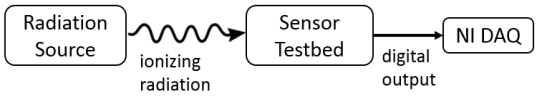

Figure 7: Schematic of characterization set-up.

their precision trade-offs will be discussed in more detail in Section V which discusses the data acquisition in detail. The node, after making a measurement, will store the results in non-volatile memory until the UAV passes over the node and sends a wake-up command to collect the data.

IV. Ultra-Low-Power Radiation Sensors

In this section, we will present the characterization of the novel radiation sensor, which is the core of the wireless sensor node. To this end, we will first explain our experimental test bed in detail, then the results obtained. These results will be used later on to determine the best parameters for our proposed energy efficient data acquisition algorithms.

A. Experimental Setup

An experimental testing chamber (Figure 8) located at the Institut de Radiophysique (ISO/IEC 17025:2005 and 17020:2012 certified) at the Centre Hospitalier Universitaire Vaudois (Lausanne, Switzerland) has been used to test the sensor, allowing the controlled irradiation of the sensor with gamma rays under well-defined dosage rate conditions. The block diagram of the experimental set up is shown in Figure 7. A radiation source (i.e., several Cs-137 sources of different radiation doses) emitted gamma rays, at four different dosage rates, on the sensor test bed. The number of pulses generated by the sensor in each test was detected and logged using a high precision National Instruments USB621X DAQ platform. This data was subsequently analyzed to determine the accuracy and precision of the fixed and dynamic window sampling algorithms.

The dosage rates (0.01, 0.01, 1 and 10 mSv/h) were selected to sweep a wide range of the characterization curve in presented in Section III-5. The exposure times were chosen to have at least 3000 pulses detected at all radiation levels to have three times more data than the recommended value of the Teviso sensor, and thus, a stable CPM reading, given the specific radiation dosage rate. The sensor was tested under standard conditions, i.e., 20 °C, 974 hPa and 23 % relative humidity. All of the results pertaining to the sensor characterization and acquisition algorithms presented in this work are based on the data acquired from these experiments.

Table I: Nominal Dosage Rates and Measured Sensor Response.

Nominal Value		Measured Value		
Radiation Dose Rate [mSv/h]	**Exposure Time [s]**	**Counted Pulses**	**Measured CPM**	**Mean Time to Settle [s]**
0.010	3399	3781	66.743	898.9
0.102	1509	9614	382.26	156.9
1.006	748	44839	3596.7	16.68
10.150	380	129190	20398	2.94

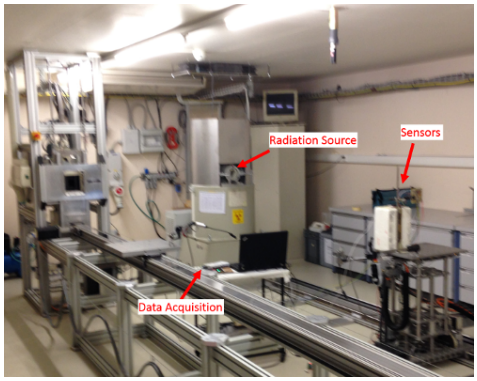

Figure 8: Laboratory set-up for radiation experiments.

B. Sensor Characterization

In order to evaluate the precision of our proposed sampling algorithms, it is necessary to first characterize the sensor's response to controlled dosage rate conditions. This characterization data will later be used to evaluate our energy-efficient data acquisition algorithm. Once the experimental setup was ready, the experiment for each dosage rate was carried out. The nominal dosage rate and CPM values calculated from the sensor response are listed in Table I. The mean time to settle is defined as the average time taken to detect 1000 pulses. As expected, the number of pulses detected per unit time increases with the radiation dosage rate. Figure 9 shows how the counts per minute (CPM) vary with the number of pulses detected, for 4 different radiation levels. These values were obtained using a sample trace of 1000 pulses for each dosage rate, which, according to the manufacturer, guarantees a stable and precise measurement. Naturally, the longer the measurement, the more precise it will be. In fact, the reference CPM column in Table I corresponds to dividing the total number of pulses detected during the experiment by the experiment's duration. This is

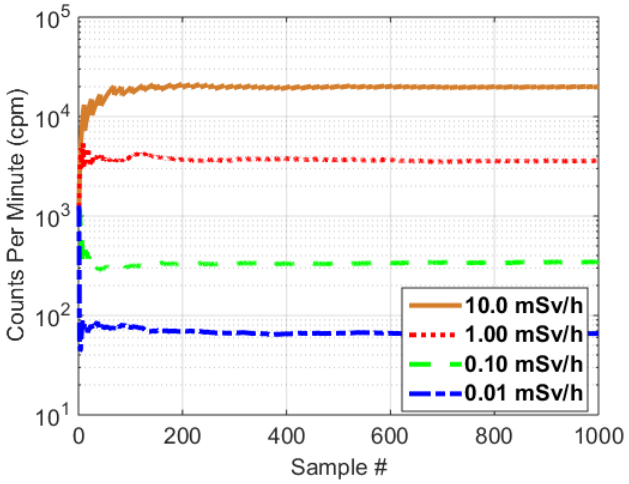

Figure 9: Measured CPM as a function of the number of samples detected, for different dosage rates.

our most precise measured value, which our proposed data acquisition algorithms will later be compared to for precision.

What is important to note is that under all four dosage rates, the measured CPM value stabilizes after 400 pulses have been detected. This is the first important observation and the foundation of our proposed approach to reduce the sampling time by counting the number of pulses detected. This will optimize a dynamic window sampling policy, since waiting for a fixed number of pulses will take shorter times at higher dosage rates, and thus reduce the energy consumed per measurement without affecting its precision. In the following section, we will explore two different data acquisition algorithms that will make a sensor reading possible within a limited amount of time.

V. Energy Optimized Sensor Data Acquisition

Due to the node's high energy efficiency requirements to achieve a self-sustainable sensor system, it is important to power manage the sensor to reduce the overall energy consumption. Duty cycling is a common way to this goal, by keeping the sensor and the node active only for a fixed amount of time within a period. Depending on the size of the active period, we can expect a certain number of pulses to be detected at a given dosage rate. Ideally, the microcontroller and the radio will spend most of their time in sleep mode and wake up only when absolutely necessary, e.g. when the sensor is activated for making a radiation measurement.

Figure 10 shows our proposed node's finite state machine. The main state, with a double outline, has the microcontroller in LPM3 mode and the sensor off. One timer is configured to periodically trigger the data acquisition phase. At the beginning of this phase, outlined in red, the microcontroller configures a timer and a counter. The first timer will generate an interrupt after a given time, called window size. The counter will simply count the number of pulses within the window size. Depending on the data acquisition algorithm, this phase can end after an interrupt from either the timer or the counter, the latter occurring if a maximum number of pulses to be detected is set. Lastly, the node enters the data transmission phase only when the WUR detects a wake-up command. The wake up command is generated by the UAV when it will be in the range of the wake up radio. At this point, the node transmits its buffered data to the UAV for further processing.

In this paper, we proposed an energy-optimized algorithm for the radiation sensor. To this end, we have taken the sensor's characterization data presented in the previous section and used it to evaluate the precision and energy efficiency with two different sampling algorithms. The first, called *Fixed Window Sampling*, will turn off the sensor after a fixed (constant) time. This method is essentially constant duty-cycling, which clearly saves power, but has some disadvantages. The second, called *Dynamic Window Sampling*, can turn off the sensor before a fixed (maximum) time if it detects a predefined number of pulses. We use the characterization data from the previous section and process it with Matlab to determine the number of pulses that would have been detected using fixed and dynamic

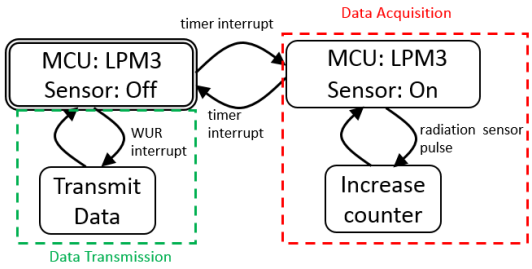

Figure 10: Node's finite state machine.

window sizes. This methodology allows us to calculate the CPM distribution for both algorithms, compare it to the known reference value, and infer the measurement's precision. To this end, the node's state machine will be discussed first, followed by the two data acquisition algorithms.

As mentioned earlier, the data acquisition phase is initiated periodically by a timer. The duration of the phase depends on the algorithm. As was shown in Table I, different dosage rates have different settling times. For the Fixed Window Sampling algorithm, if we were to choose a high enough window value, we guarantee that we will obtain a precise measurement for a wide range of radiation levels. This, however, is very inefficient in terms of energy since higher levels of radiation exhibit much shorter settling times. With this characteristic in mind, we propose the second algorithm, which will keep the sensor on until either a maximum time has elapsed, or a given number of pulses has been detected. By turning off the sensor after the reading has stabilized, the energy consumed by the sensors can be significantly reduced, particularly at high levels of radiation, which have short stabilization times. In the next subsection, the two algorithms will be discussed in greater detail.

A. Fixed Window Sampling

In the Section IV, we have analyzed the radiation sensor's response to different dosage rate conditions. It has been determined that after only 400 pulses were detected, the CPM measurement had a stable value. However, as it had been shown in Table I, waiting for 400 pulses at low dosage rates would take prohibitively long measurement times. For this reason, and given our high radiation application scenario, we have chosen a maximum window of 20 s, which will result in accurate readings at high dosage rates while still able to detect low levels with an acceptable precision, as can be seen in the "avg. CPM dispersion" column in Table II. These values were obtained by counting the number of pulses detected within fixed time windows of 20 s. The average CPM dispersion indicates how consistent the fixed window reading was compared to the Reference CPM value, our precise reference value. We define the dispersion in the following way: Let M_{CPM} be a vector containing the CPM values from all 20 second fixed window measurements from our characterization data. In order to calculate the dispersion D, we use the following formula:

$$D = 100 \cdot \frac{mean(M_{CPM} - stddev(M_{CPM}))}{mean(M_{CPM})} \quad (1)$$

Table II: Sensor Response with Fixed Window = 20 sec.

Radiation Dose Rate (mSv/h)	Average CPM	Avg. CPM Dispersion [%]
0.010	66.800	7.93
0.102	382.50	4.03
1.006	3598.0	1.37
10.150	20330	0.33

The dispersion is a measure of how different the value from one measurement varies to the next. If, for example, the sensor generated pulses perfectly periodically, the measured CPM values would be the same, meaning the dispersion would be zero. Unfortunately, the pulse generation depends directly on the ionizing radiation, and is inherently random. This means that even when the radiation level is kept constant, for small time windows, the measurement might give slightly different results. In fact, for a dosage rate of 0.010 mSv/h, for example, the dispersion is 7.93 % of the expected CPM value, while at 10.0 mSv/h, the dispersion is only 0.33 %. This result is to be expected, since the lower dosage rate will have a lower number of detected pulses within the fixed time window, and the CPM value has not yet fully stabilized. Figure 11 shows the average number of pulses detected in all measurements of a given window size in a semi-log plot. Naturally, with higher dosage rates, a much greater number of pulses are detected within a fixed window size. Due to this difference in the number of pulses, the measurement's precision within a fixed window will depend on the dosage rate. Figure 12 shows the maximum error for different dosage rates in fixed window measurements as a function of the window size. In order to calculate the maximum error E, we use the following formula:

$$E = 100 \cdot \frac{max|CPM_{ref} - M_{CPM}(window)|}{CPM_{ref}} \quad (2)$$

Where CPM_{ref} represents the most precise CPM value, and M_{CPM}(Window) is a vector containing all the measurements of a given window size. The CPM_{ref} values are listed under the "Measured CPM" column in Table I. As expected, the maximum error converges to zero with increasing window size. The only difference between the lines is the time scale: for lower dosage rates, the stabilization times are longer. It should be noted that there are two types of imprecise readings: The first, which goes up to 100%, happens at low dosage rates with very small time windows. In this scenario, a fixed window measurement will not detect any pulses, resulting in a 0 CPM reading, or 100% error. The second type of imprecision occurs with higher dosage rates and small window sizes. Here, a quick burst of pulses can lead to an artificially higher reading, which can lead to errors above 100%. From this result, we can determine that a fixed window duration of 20 s can offer high precision reading at high dosage rates, and an acceptable precision at lower rates.

B. Dynamic Window Sampling

As presented in the previous subsection, a fixed (periodic) window size can by itself reduce the energy consumed by the sensor compared to continuous sampling. Furthermore, it has been shown that a given fixed size has a variable precision, which depends on the dosage rate: Higher dosage rates have a higher number of pulses detected within the same time, and thus a more stable CPM reading. The aim of the second algorithm is to explore a more energy efficient data sampling algorithm that can reduce the window size for high dosage rates, such that the sampling ends after a stable CPM reading can be calculated. From Section IV, it has been shown that after a few hundred pulses have been detected, a stable measurement can be obtained. From our empirical data, it was determined that with a threshold of 400 pulses, we can significantly reduce the window sizes with only a marginal effect on the maximum measured CPM error. We once again utilize the characterization data acquired at our testing facility, and based on that, we calculate all the dynamic window measurements, to then determine what the longest windows sizes are and what the maximum error for those measurements are. These results are shown in Figure 15. The blue bars show the maximum measured window size for different radiation levels. For lower levels of radiation, this window size will be our predefined maximum, 20 s. This is expected because at low levels of radiation, it takes a relatively long amount of time to reach 400 pulses. As the level of radiation increases, however, this stabilization time decreases, and already for 1 mSv/h, we detect a maximum window of 6 s. This 70% reduction in window size leads to significant savings in the sensor energy. Furthermore, the higher the radiation levels are, the higher are the potential savings: at 10 mSv/h the maximum window size was 1.5 s, or a 92.5 % window size reduction. Since the energy spent per measurement is proportional to the window size, this reduction in window size is equivalent to a reduction in the energy spent per measurement. The red bars show the maximum error for a measurement at a given radiation level. Note how the error decreases as the radiation level increases. This is expected since a time window of 20 s is not long enough for a precise measurement at low levels of radiation at high levels, a relatively short amount of time necessary to reach the 400 pulses we have selected as the

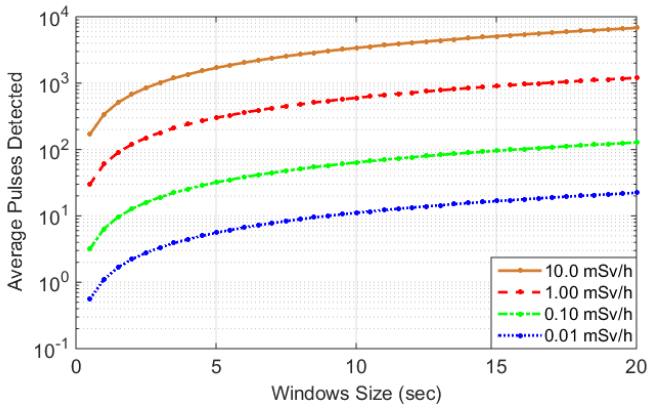

Figure 11: Average number of pulses detected as a function of the window size and dosage rates.

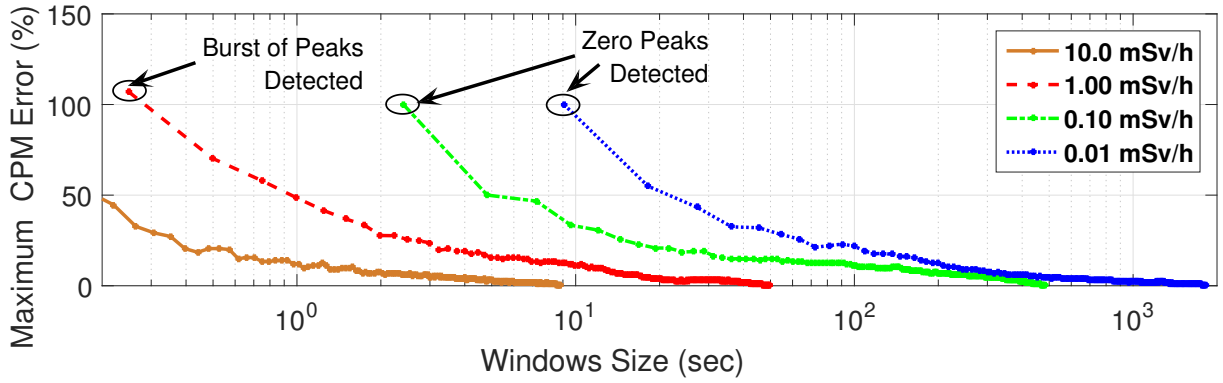

Figure 12: Maximum CPM error measured with fixed window sampling as a function of the window size, for different dosage rates.

threshold for a precise measurement.

C. Self-Sustainability Model

In this section, we introduce the self-sustainability model of our application scenario to evaluate the proposed approach, with a special focus on the benefits of the adaptive sampling algorithm and wake up radio capabilities in the communication. In all current scenarios, the WUR will detect the request for data retrieval from the UAV and trigger the data transmission once per hour. As presented in Figure 10, the sensor nodes will make a measurement periodically and store the data until a transmission request from a UAV is detected. During the data acquisition (DAQ) phase, the fixed and dynamic window sampling will count the number of pulses within a maximum time frame to calculate the CPM. During the transmission (TX) phase, the CC110L radio is activated to transmit the data stored in the node. Since a WUR is being used, there is no need for any polling. It is designed to be always listening for the wake-up request. This comes at the cost of a slight increase in the idle power, in the order of one microwatt. Thus, the energy consumption for both methodologies (fixed and dynamic windows) can be summarized in the following equations:

$$E_{Consumed,WUR} = E_{DAQ} + E_{TX} + E_{idle\_wur} \quad (3)$$

Where E_{DAQ}, E_{TX}, and E_{Idle_wur} are the node's periodic energy consumption from the data acquisition, data transmission, polling and idle phases, respectively. The nano-watt WUR is an important component in reducing the node's power consumption, since it allows the other components to be in sleep mode and generates an interrupt only when needed. However, minimizing a node's power consumption alone is not enough to reach self-sustainability. Energy harvesting is necessary to replenish the available energy for uninterrupted operation. In our application scenario, the solar panel will harvest energy from the available sunlight, which varies with time. Within a period, the difference in energy can be expressed as follows:

$$\Delta E_{Period} = E_{Harvested} - E_{Consumed} \quad (4)$$

In systems with energy storage, ΔE can either be positive or negative. If it is positive, it means more energy was harvested than consumed. As a result, the amount of stored energy will increase. On the other hand, if the ΔE is negative, it means more energy was consumed than harvested, and the amount of stored energy will decrease.

$$E_{storage}(t + Period) = E_{storage}(t) - \Delta E_{Period}(t) \quad (5)$$

Where $E_{Storage}(t)$ and $E_{Storage}(t+Period)$ are the energy storage levels at the time t and t + Period. Since the storage element has a limited capacity, E_{Max}, the storage level cannot surpass it. On the other hand, $E_{Storage}$ has to guarantee that there will always be enough energy to acquire and transmit data when necessary, otherwise data can be lost, and the node will no longer be self-sustainable. This minimal value, E_{Min}, is simply $E_{Consumed}$. Therefore, at any time t, the following equation has to be satisfied:

$$E_{max} > E_{store}(t) > E_{mean} \quad (6)$$

VI. Experimental Results

In this section we will present and discuss the experimental results of our data acquisition algorithms and energy sustainability models. As was shown in Section 3, our energy budget is given by EH and energy storage. To allow the whole system to be self-sustainable, this budget must be large enough for our application requirements. To this end, we carried out power measurements of the sensor node during its different states and intake energy from Sanyo's AM-1417 solar panel (11.7mm x 35.0mm) during several days. These measurements have been used in our simulation using the model presented in previous section to demonstrate the viability and self-reliability of the proposed solution.

A. Power Consumption Measurements and Intake Energy

As the low power is crucial to achieve a self-sustainable system, the first step has been to evaluate the power consumption measurement of the designed and developed node. Table III shows the sensor node's power consumption with a 3.3V power

Table III: Node's Power and Timing Characteristics Per Hour.

Node Phase	Description	Avg. Power [mW]	Time [s]
Single Data Acquisition (DAQ)	MSP430 in LPM3, CC110L in sleep	1.731	Max 20
Data Transmission (TX)	MSP430 active, CC110L in TX	23.1	0.020
Idle_wur	MSP430 in LPM3, CC110L in sleep + WUR	0.031	Max. 3598.5

supply and with the microcontroller running at 8 MHz. During the DAQ phase, the MSP430 is in low-power mode LPM3, and both a timer and counter are used to measure time and register the detected pulses from the radiation sensor.

During the TX phase, the main radio is turned on and used to transmit data back to the UAV. Data transmission is the most power hungry phase, consuming 23.1 mW, and lasting approximately 20 ms to send 60 bytes, which is the data corresponding to 1 hour. Due to the presence of the WUR, the node can enter an ultra-low power idle_wur phase, in which the WUR awaits a transmission request. In this state, the node consumes only 30 μW + 1 μW from the MCU and the WUR, respectively.

Figure 13 shows the experimental measurement from our selected solar panel in an outdoor environment during 6 days. The figure shows how the amount of sunlight can vary the available power considerably during the day, due to unpredictable weather conditions. The peak harvester power is only of few mW due mainly to the small size of the solar panel. This makes the power management and the energy efficient acquisition algorithms even more important and challenging.

B. Wake-Up Radio Communication In-field Experiments.

To evaluate the range of the energy efficient protocol using the wake up radio in the outdoor scenario, we have carried out a set of measurements using a transmitter and a wake up radio. The experimental set up includes the following hardware components: i) the wake up radio with -55dBm sensitivity equipped with a commercial 900MHz antenna with +3dBi gain. ii) A demo board with an MSP430 microcontroller and a CC110L transceiver has been deployed in the field to different distances from 5 meters to 40 meters in a country side area with steps of 5 meters. The antennae have been placed 1 meter above the ground. For each step of 5 meters, 1000 wake up beacons of 5 consecutive bit '1' has been transmitted and the log of the received data has been traced. The transmission power of the CC110L has been set to a fixed value of +10dBm. With this configuration, we could measure the influence of the distance on the packet loss and identify the safe region where data are always received correctly.

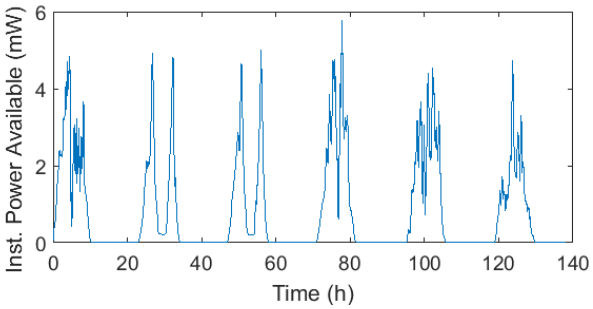

Figure 13: Instantaneous power available measured in an outdoor environment.

The performance in terms of packets received and false positive wake up are presented in Table IV. It can be noticed that up to 30 meters, the packets success rate is above the 99 % so the communication can be considered accurate. As the range starts to increase, the success rate decreases to 75 %. It is interesting to notice that the false positives are very rare. This heavily depends on the environment, and because of our radioactively contaminated scenario, a very low level of radio frequency noise is expected. Moreover, if the environment becomes noisy or a more robust signal is needed, the wake up radio communication can provide both addressing capability or the length of the wake up beacon can be increased.

Table IV: Performance of distance vs packet lost for 100 wake up beacons.

Distance	Packets	Received	False Positive
5 meters	1000	1000	0
10 meters	1000	1000	1
15 meters	1000	1000	0
20 meters	1000	1000	1
25 meters	1000	999	0
30 meters	1000	999	0
35 meters	1000	978	0
40 meters	1000	756	1

C. Simulation and Self-Sustainability

In order to demonstrate the self-sustainability of our proposed solution, the above-presented measurements have been used as input to our Matlab simulation. Based on the model presented in Section 6, it calculates the energy storage level for fixed and dynamic window sizes and sampling periods. It should be noted that we do not consider leakage currents or temperature/aging degradation in the supercapacitor. The former is negligible compared to the node's sleep power, and the former is mitigated by over-dimensioning. The first aim of this simulation is to evaluate the benefit between the fixed windows, dynamic windows and continuous sampling. As a second aim we wanted to highlight the importance of the wake up radio. Figure 14 shows how the sensor node would operate under the energy harvesting conditions presented in Figure 13. There are four lines, representing the energy storage level for fixed windows, dynamic windows and continuous sampling when exposed to a dosage rate of 10 mSv/h. The blue line indicates the energy storage level when the sensor is continuously acquiring data. As expected, this is very expensive in terms of energy and

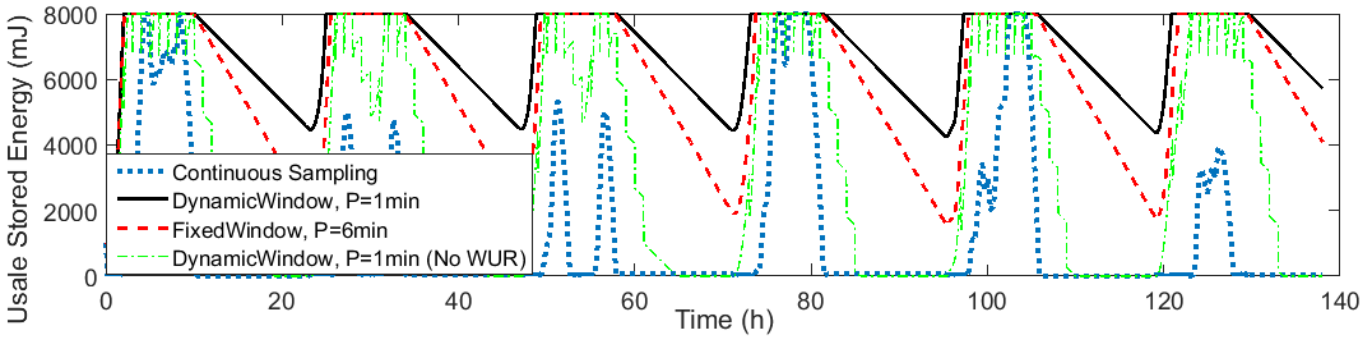

Figure 14: Energy storage levels for Fixed and Dynamic Window Sampling with different periods, at dosage rate=10mSv/h.

cannot satisfy the requirement of continuous monitoring as the storage device is completely depleted for long periods of time. In fact, there is stored energy only during periods of excess power during the day.

The red line represents sampling with a fixed window size of 20 s and a sampling period of 6 minutes. It is interesting to notice, for Fixed Window Sampling, that the stored energy level is the same, regardless of the environmental dosage rate. At its lowest level, there are 1954 mJ stored in the supercapacitor, indicating that even with our initial sampling algorithm, our proposed node exhibits self-sustainable behavior. The black line represents the storage levels for dynamic window sizes with a sampling period of 1 minute. Since the dosage rate is the maximum, this energy efficient algorithm will have a reduced window size of only 1.5 s, as shown in Figure 15. Because of this reduced energy, the system can support the elevated sampling rate, and still maintains at least 4477 mJ stored in the supercapacitor at all times. This corroborates the energy savings introduced by our proposed data acquisition algorithm at high dosage rates. In fact, as Table V shows, up to 92.5 % of the energy per sample can be saved using our proposed algorithm.

These energy savings come at small price of precision.

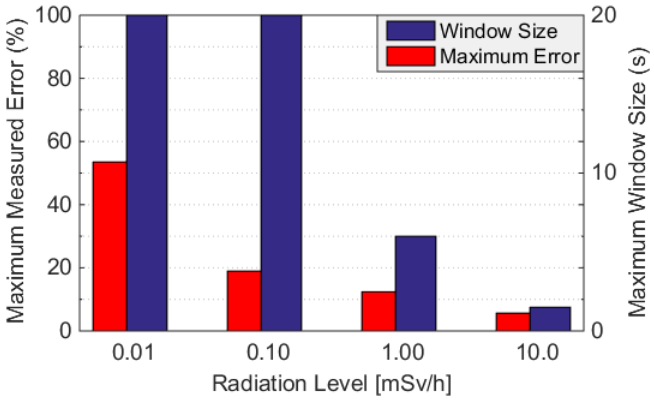

Figure 15: Maximum detected error with dynamic window sizes (Max. Window=20 s, Pulses=400) for different dosage rates.

For high dosage rates, fixed window sampling can offer a maximum error of less than 1.4 % for 1.006mSv/h, while dynamic windows have a maximum error of 12.39 %. Lastly, the green line corresponds to the scenario where there is no wake-up receiver. Here, the main radio needs to perform polling, which we have defined as lasting for 1 minute every hour, so the node can detect the presence of the UAV when it passes over the node. This strategy is clearly energy inefficient, since the main radio is the most power consuming component, and as a result, the node has no stored energy for considerable periods of time.

These simulations confirm the energy efficiency of the proposed data acquisition, dynamic power management and wake-up receiver. These features allow the node to make radiation dosage measurements with high sampling frequency and precision, while guaranteeing the node's self-sustainability.

VII. Conclusions

This work has presented a self-sustainable radioactive sensor node for environmental monitoring in hazardous environments. A novel off-the-shelf low power radiation sensor has been presented and characterized in detail, and two energy efficient data acquisition algorithms have been proposed. The proposed sampling methods have been evaluated under several different radiation dosage rates in terms of precision and energy saving using real-world measurements. The whole node has been designed to have a small form factor, low power and self-sustainability, enabling it to be distributed by UAVs across inaccessible areas. In some cases it might not only be dangerous for a human to perform measurements, it might not even be possible. The node contains solar panels and a supercapacitor, which enables it to gather enough energy for continuous periodic sensing. Furthermore, with the combination of a power efficient acquisition algorithm, an ultra-low power

Table V: Summary of Dynamic Window Sampling Results.

Radiation Dose Rate (mSv/h)	Dynamic Window Size [s]	Energy Savings per sample [%]	Max. CPM Error (%)
0.010	20	0	53.53
0.102	20	0	18.97
1.006	6	70	12.39
10.150	1.5	92.5	5.63

WUR and radio transceiver, the node is able to transmit its sensed data back to the UAV with very high energy efficiency. As a result, the proposed solution is able to produce and continuously update an accurate map of radioactivity levels in industrial accident sites. The power measurements demonstrate the viability of a self-sustainable node with dynamic window sampling and the benefits of using a combination of aggressive power management and low power techniques. The results show that with a WUR and our proposed sampling algorithm, the node achieves the self-sustainability level with low latency transmissions, providing measurements with fine-grained time resolution and high precision. The experimental results show that even with low energy budgets, our low power HW/SW codesign with novel sensors can enable the perpetual monitoring of dangerous areas.

VIII. Acknowledgments

This work was supported by "Transient Computing Systems", a SNF project (200021_157048), and ETH Zürich Grant funding. The authors would also like to express their gratitude to CHUV and Teviso Sensor Technologies Ltd. for their assistance during the preparation of this manuscript. The very helpful feedback from the anonymous reviewers is greatly appreciated.

References

[1] J. Saegusa *et al.*, "Observation of fallout deposition in an outdoor swimming pool 50 km away from the fukushima daiichi nuclear power plant," *Radiation Measurements*, vol. 60, pp. 53–58, 2014.

[2] L. M. Oliveira *et al.*, "Wireless sensor networks: a survey on environmental monitoring," *Journal of communications*, vol. 6, no. 2, pp. 143–151, 2011.

[3] M. Srbinovska *et al.*, "Environmental parameters monitoring in precision agriculture using wireless sensor networks," *Journal of Cleaner Production*, vol. 88, pp. 297–307, 2015.

[4] W. Du *et al.*, "Sensor placement and measurement of wind for water quality studies in urban reservoirs," *ACM Transactions on Sensor Networks (TOSN)*, vol. 11, no. 3, p. 41, 2015.

[5] R. J. Nemzek *et al.*, "Distributed sensor networks for detection of mobile radioactive sources," *Nuclear Science, Transactions on*, vol. 51, no. 4, pp. 1693–1700, 2004.

[6] S. M. Brennan *et al.*, "Radioactive source detection by sensor networks," *Nuclear Science, Transactions on*, vol. 52, no. 3, pp. 813–819, 2005.

[7] Y. Wang *et al.*, "Robot-assisted sensor network deployment and data collection," in *Computational Intelligence in Robotics and Automation, 2007. CIRA 2007. International Symposium on*. IEEE, 2007, pp. 467–472.

[8] F. G. Costa *et al.*, "The use of unmanned aerial vehicles and wireless sensor network in agricultural applications," in *Geoscience and Remote Sensing Symposium (IGARSS), 2012 IEEE International*. IEEE, 2012, pp. 5045–5048.

[9] A. Gomez *et al.*, "Self-powered wireless sensor nodes for monitoring radioactivity in contaminated areas using unmanned aerial vehicles," in *Sensors Applications Symposium (SAS), 2015 IEEE*. IEEE, 2015, pp. 1–6.

[10] M. F. Lagadec *et al.*, "Dēta no takkyūbin (dnt) – data delivery service," in *International Contest of Applications in Nano-Micro Technologies (iCAN)*, July 2014.

[11] Y. Wu *et al.*, "Energy-efficient wake-up scheduling for data collection and aggregation," *Parallel and Distributed Systems, IEEE Transactions on*, vol. 21, no. 2, pp. 275–287, 2010.

[12] J. P. Amaro *et al.*, "Harvested power wireless sensor network solution for disaggregated current estimation in large buildings," *Transactions on Instrumentation and Measurement*, 2015.

[13] E. Sardini *et al.*, "Self-powered wireless sensor for air temperature and velocity measurements with energy harvesting capability," *Instrumentation and Measurement, Transactions on*, vol. 60, no. 5, pp. 1838–1844, 2011.

[14] A. S. Weddell *et al.*, "A survey of multi-source energy harvesting systems," in *Proceedings of the Conference on Design, Automation and Test in Europe*. EDA Consortium, 2013, pp. 905–908.

[15] S. Akbari, "Energy harvesting for wireless sensor networks review," in *Computer Science and Information Systems (FedCSIS), 2014 Federated Conference on*. IEEE, 2014, pp. 987–992.

[16] A. Gomez *et al.*, "Dynamic energy burst scaling for transiently powered systems," in *Proc. DATE Conf.* EDA Consortium, 2016, pp. 349–354.

[17] ——, "Wearable, energy-opportunistic vision sensing for walking speed estimation," in *Proc. SAS Symp.* IEEE, 2017, pp. 1–6.

[18] R. Yan *et al.*, "Energy-aware sensor node design with its application in wireless sensor networks," *Instrumentation and Measurement, IEEE Transactions on*, vol. 62, no. 5, pp. 1183–1191, 2013.

[19] M. Magno *et al.*, "Wake-up radio receiver based power minimization techniques for wireless sensor networks: A review," *Microelectronics Journal*, vol. 45, no. 12, pp. 1627–1633, 2014.

[20] ——, "Combination of hybrid energy harvesters with mems piezoelectric and nano-watt radio wake up to extend lifetime of system for wireless sensor nodes," in *Architecture of Computing Systems (ARCS), Proceedings of 2013 26th International Conference on*. VDE, 2013, pp. 1–6.

[21] ——, "Ensuring survivability of resource-intensive sensor networks through ultra-low power overlays," *Industrial Informatics, IEEE Transactions on*, vol. 10, no. 2, pp. 946–956, 2014.

[22] D. Gascon *et al.*, "Wireless sensor networks to control radiation levels." Libelium Communicaciones Distribuidas, 2011.

[23] R. Gomaa *et al.*, "Zigbee wireless sensor network for radiation monitoring at nuclear facilities," in *Wireless and Mobile Networking Conference (WMNC), 2013 6th Joint IFIP*. IEEE, 2013, pp. 1–4.

[24] "Teviso sensor technologies. nuclear radiation sensor rd3024 datasheet," Rev. 19.12.2014.

[25] N. Bui *et al.*, "Staying alive: System design for self-sufficient sensor networks," *ACM Transactions on Sensor Networks (TOSN)*, vol. 11, no. 3, p. 40, 2015.

[26] P. Corke *et al.*, "Autonomous deployment and repair of a sensor network using an unmanned aerial vehicle," in *Robotics and Automation, 2004. Proceedings. ICRA'04. 2004 IEEE International Conference on*, vol. 4. IEEE, 2004, pp. 3602–3608.

[27] J. Liang *et al.*, "A survey of coverage problems in wireless sensor networks," *Sensors & Transducers*, vol. 163, no. 1, 2014.

[28] Y.-T. Huang *et al.*, "Adaptive drone sensing with always return-to-home guaranteed," in *Proceedings of the 1st International Workshop on Experiences with the Design and Implementation of Smart Objects*, ser. SmartObjects '15. New York, NY, USA: ACM, 2015, pp. 7–12. [Online]. Available: http://doi.acm.org/10.1145/2797044.2797054

[29] G. Tuna *et al.*, "An autonomous wireless sensor network deployment system using mobile robots for human existence detection in case of disasters," *Ad Hoc Networks*, vol. 13, pp. 54–68, 2014.

[30] M. Magno *et al.*, "An ultra low power high sensitivity wake-up radio receiver with addressing capability," in *Wireless and Mobile Computing, Networking and Communications (WiMob), 2014 IEEE 10th International Conference on*. IEEE, 2014, pp. 92–99.

[31] D. Spenza *et al.*, "Beyond duty cycling: Wake-up radio with selective awakenings for long-lived wireless sensing systems," in *Proc. INFOCOM*, 2015.

[32] V. Jelicic *et al.*, "Analytic comparison of wake-up receivers for wsns and benefits over the wake-on radio scheme," in *Proceedings of the 7th ACM workshop on Performance monitoring and measurement of heterogeneous wireless and wired networks*. ACM, 2012, pp. 99–106.

[33] F. Sutton *et al.*, "Zippy: On-demand network flooding," in *Proceedings of the 13th ACM Conference on Embedded Networked Sensor Systems*. ACM, 2015, pp. 45–58.

[34] M. Magno *et al.*, "Design, implementation, and performance evaluation of a flexible low-latency nanowatt wake-up radio receiver," *IEEE Transactions on Industrial Informatics*, vol. 12, no. 2, pp. 633–644, 2016.

[35] J. Prekeges *et al.*, *Nuclear medicine instrumentation*. Jones & Bartlett Publishers, 2012.